Experimental and Computational Modelling for Optimised Biodiesel Production from Waste Ram Fat Using a Kaolinite-Clay and Eggshell-Derived Catalyst

E.O. Ajala[1*], A.B. Ehinmowo[2], A.D. Oladipupo[3], S. Opawoye[1], A.M. Ndana[4], and D.A. Ariyoosu[5]

[1]Department of Chemical Engineering, University of Ilorin, Ilorin, Kwara State, Nigeria.
[2]Department of Petroleum and Gas Engineering, University of Lagos, Lagos State, Nigeria.
[3]Department of Chemical Engineering, University of Michigan, Ann Arbor, USA.
[4]Department of Chemical Engineering, Federal Polytechnic, Bida, Nigeria.
[5]Department of Business Law, Faculty of Law, University of Ilorin, Ilorin, Kwara State, Nigeria.

ABSTRACT: Efficacy of some optimisation techniques for biodiesel production were studied for the transesterification of waste ram fat (WRF) with an activated kaolinite-clay/chicken-eggshell (AKC-CE) catalyst. The optimisation study focused on the design of the experiment through response surface methodology by I-optimal experimental design, algorithms (Particle Swamp Algorithm (PSO), Firefly Optimisation (FO) and Genetic Algorithm (GA)) and machine learning (Artificial Neural Network (ANN)). The biodiesel produced was characterised by its Fatty Acid Methyl Esters (FAME) composition using a Gas Chromatography Mass Spectrophotometer (GC-MS). Among the models investigated, the GA, and FA outperformed the others, as they predicted the highest biodiesel yield of 99.00% and experimentally validated as a 99.24% yield. This optimum yield was attained at the optimal input variables of methanol: oil molar ratio (10.33 w/w), reaction time (2.33 h), reaction temperature (95^{o}C), and catalyst quantity (6.44%, w/w). The GCMS accounted for 97.42% of FAME composition at the same optimal input variables. Thus, the research validates the usage of modern algorithms in exploring the best operating conditions to achieve optimum biodiesel yield. The fuel properties obtained confirmed the suitability of the biodiesel produced as an alternative to diesel. This research concludes that the AKC-CE has potential application for optimum yield of biodiesel production.

KEYWORDS: Response Surface Methodology; Particle Swamp Algorithm; Firefly Optimisation; Genetic Algorithm.

[Received Jan. 24, 2025; Revised Feb, 26, 2025; Accepted Mar. 3, 2025] Print ISSN: 0189-9546 | Online ISSN: 2437-2110

I. INTRODUCTION

The search for alternative fuels has inspired and intensified scientific efforts to develop feasible biofuels that can replace or reduce the use of fossil fuels (Antonio et al., 2018). This is due to spiraling fossil fuel prices, snowballing energy demand because of industrialisation, and the environmental pollution caused by its utilisation. Biodiesel, also known as fatty acid methyl esters (FAME), is a mono-alkyl ester of long-chain fatty acids produced through the transesterification of vegetable oil or animal fat with alcohol in the presence of a catalyst (Ighose et al., 2017). Biodiesel utilisation has gained increased attention because it is non-toxic, nearly carbon-neutral, and free of sulphur and aromatic compounds compared to petroleum-derived diesel which makes it a suitable alternative to fossil fuels (Ajala et al., 2022). However, its higher production cost than fossil fuel products remains a significant barrier to widespread adoption (Odetoye et al., 2021). The production costs are largely attributed to the feedstock of vegetable oil or animal fat (70.6%), catalysts (12.6%), and other factors (16.8%) (Linganiso et al., 2022). The significance of feedstock as the primary contributor to production expenses necessitates the identification of affordable triglyceride (TG) sources that do not interfere with food crops to mitigate biodiesel production costs (Odetoye et al., 2021). The production of environmentally and economically sustainable biodiesel has consequently emerged as a matter of great importance (Hasan & Ratnam, 2022; Toldra-Reig et al., 2020). Various waste animal fats have been utilised as feedstock in the production of biodiesel such as tallow (Banković-Ilić et al., 2014), lard (Sarantopoulos et al., 2014) and chicken fat (Odetoye et al., 2021). However, the presence of high free fatty acid (FFA) and moisture content in the WRF which promotes soap formation instead of biodiesel is the challenge militating its deployment as a suitable feedstock for biodiesel production. Another drawback is the difficulty in catalyst separation from the product which results in low biodiesel yield and high cost of production, especially when a homogeneous catalyst is used (Mandari & Kumar, 2022).

Optimisation of the transesterification process of TG is essential in biodiesel production as it generally involves a trade-off between alcohol molar ratio, reaction time, temperature and catalyst quantity. This is to obtain a higher activity, selectivity and longer catalyst lifetime (Albuquerque et al., 2008). In recent times, central composite design (CCD) aided response surface methodology (RSM) was regularly used to investigate the combined effects of many process parameters. The task was accomplished through the experimental design, model development, and identification of optimal parameters with a notable level of precision. In the context of decision-making problems that involve conflicting objectives, the RSM poses certain limitations due to its reliance on the maximisation of biodiesel yield which is a prominent

*Corresponding author: ajala.oe@unilorin.edu.ng *doi:* http://dx.doi.org/10.4314/njtd.v22i1.3322

constraint in real-world scenarios (Hajra et al., 2015). In addition, to maximise biodiesel yield, minimisation of reaction time can aid the optimisation of biodiesel yield; these two goals are intrinsically incompatible as it is problematic to increase biodiesel yield simultaneously with minimising reaction time. Therefore, the optimal process parameters should be chosen in such a way that the highest feasible throughput, that is, biodiesel yield (first objective function) is obtained when the reaction time is minimised (second objective function) (Hajra et al., 2015). With these in mind, biodiesel production is an outstanding candidate for a multi-objective optimisation process. Among the multi-objective optimisation powerful tools, Artificial Neural Networks (ANN), and meta-heuristics algorithms (Genetic Algorithm (GA), Particle Swamp Optimisation (PSO) and Firefly Algorithm (FA)) were selected for this study. The details about the applications and merits of ANN and meta-heuristic algorithms (PSO, GA, and FA) have been well discussed in the literature (Coello et al., 2007; Sadeghiram, 2017; Tsai et al., 2004). It is important to note that the application of RSM and ANN in biodiesel production modelling alongside other meta-heuristic algorithms, is a seldom discussed topic within the existing literature. The transesterification process is a complex biochemical reaction, and many kinetic models rely on simplified assumptions about molecular interactions, which may not accurately reflect the intricacies of real-world systems. Modelling this phenomenon using chemical kinetics and optimising yield involves several challenges. Key assumptions, such as predefined chemical reaction pathways, may overlook the diversity of potential pathways the reaction could follow. Moreover, transesterification involves multiple reaction steps, making it difficult to accurately identify the rate-determining step and effectively model the entire mechanism. To address these complexities, additional assumptions such as pseudo-steady-state approximations or rate-determining step considerations are often required. However, such simplifications may limit the model's ability to describe the reaction dynamics comprehensively.

Therefore, this study aimed to maximise biodiesel yield and minimise process conditions such as alcohol molar ratio, reaction time, temperature, and catalyst quantity, through data-driven techniques which is novel. Response Surface Methodology (RSM) and Artificial Neural Networks (ANN) were used for modelling the process as $Y=f(X_1, X_2, X_3, X_4)$, and algorithms such as FA, GA, and PSO were applied to determine fitting parameters (a, b, c, …). The objective function minimises the mean squared difference between the actual and estimated Y values, which mitigates the risks of errors and enhances the robustness of the results. Also, the biodiesel produced was characterised to determine its FAME composition using a Gas Chromatography-Mass Spectrophotometer (GC-MS).

II. METHODOLOGY

A. Biodiesel Production using AKC-CE Catalyst

The AKC-CE catalyst used in this study was developed and reported in a previous work (Ajala et al., 2024). The transesterification of biodiesel production was carried out in a 500 ml three-neck flask equipped with a water-cooled reflux condenser, thermometer and magnetic stirrer. The WRF of 10 kg and methanol: oil ratio of 6:1 was charged into the flask with 1 g of AKC-CE catalyst (10%, w/w of catalyst to WRF). The reaction was set up by continuously stirring the mixture at 600 rpm for 4 h at a temperature of 70°C. Subsequently, the catalyst was recovered through filtration using filter paper and the liquid phase was transferred into a 150 ml separating funnel for 24 h. This was to separate the lower glycerol layer from the upper FAME which is biodiesel. The excess methanol was recovered from the upper layer through a rotary evaporator and the biodiesel yield was calculated using Equation 1:

$$\%Yield\ of\ biodiesel = \frac{Weight\ of\ biodiesel\ recovered}{Weight\ of\ WRF\ used}\ x\ 100 \quad (1)$$

B. Experimental Design, and Model Analysis for Biodiesel Yield

Response surface methodology

To evaluate the efficiency of the AKC-CE catalyst in the transesterification of the WRF, an I-optimal experimental design of Design Expert (version 10.0.1.0) was employed for the optimisation study. This was considered at three-level-four factors as shown in Table 1, which are MeOH: oil mole ratio (12:1 – 18:1), reaction time (2 – 4 h), temperature (70 - 90^{o}C), and catalyst quantity (5 – 15 wt%). Four main analytical steps: analysis of variance (ANOVA), significance test, multiple regression analysis and the plotting of response surface were performed to establish the quality of the fitted cubic response model shown in Equation 2:

$$Y(x) = \beta_0 + \sum_{i=1}^{q} \beta_i x_i + \sum\sum_{i<j=2}^{q} \beta_{ij} x_i x_j + \sum\sum\sum_{i<j<k=3}^{q} \beta_{ijk} x_i x_j x_k + \varepsilon \quad (2)$$

Where $Y(x)$ = Response variable (Biodiesel yield), β_0 = constant term, q = number of variables, β_i = linear coefficients, β_{ij} and β_{ijk} = interaction coefficients, x_i, x_j and x_k = process variables and ε is the residual.

The predicted values obtained from the RSM model were compared with the actual values to evaluate the model's performance. The experimental data obtained using the optimal condition from the mathematical model were also used as a validating set and compared with the predicted values.

Table 1: Experimental design-build information

File version	**10.0.1.0**			
Study Type	**Response surface**	Subtype	Randomised	
Design Type	**I-optimal**	Coordinate Exchange	**Runs**	**41**
Design Model	**Cubic**	**Build time (ms) 2833**		
Factor	**Name**	**Units**	**Minimum**	**Maximum**
A	MeOH: oil molar ratio	w/w	12.00	18.00
B	Reaction time	H	2.00	4.00
C	Reaction Temperature	^{o}C	70.00	90.00
D	Catalyst quantity	w/w, %	5.00	15.00

Artificial neural network (ANN)

The ANN modelling of the process conditions to optimise biodiesel yield was implemented using multilayer feedforward neural networks. This was performed using MATLAB version 2021 which comprised a neural network toolbox with embedded Levenberg-Marquardt with other key features shown in Table 2.

Table 2: ANN model parameters

ANN Model Parameter	**Value**
Number of Neurons	10
Number of layers	2
Network Type	Feed-forward backprop
Epoch	1000
Number of validation checks	6

The ANN architecture comprises an input layer with four neurons and an output layer with one neuron. The neurons for the input layer are MeOH: oil molar ratio, reaction time, reaction temperature, and catalyst quantity while that of the output layer is the percentage yield of biodiesel. The neurons in the hidden layer are set to sum up the weighted inputs with the related bias using Equation 3a, to direct the input data towards a more non-linear system (Betiku et al., 2016). To formulate the activation function of the input and output layers, the hyperbolic tangent sigmoid transfer function (tansig), and pure-linear transfer function (purelin) were selected, respectively, using Equation 3b. Equation 3c was employed to determine the net input to the node in the output layer. Iterative testing of several neural networks was used to identify the number of hidden neurons until the output's mean square error (MSE) value was minimised. The data set was divided into two subsets; the training set (60%), and the

testing set (40%). This was done to assess the ANN's generalisation capacity and the model's ability to predict hidden data not utilised for training.

$$x_j = \sum_{i=1}^{p} y_i\, w_{ji}^{in} + b_j^{in} \quad (3a)$$

$$(x) = tansig(x) = \frac{1-e^{-x}}{1+e^{-x}} \quad (3b)$$

$$y_k = \sum_{j=1}^{q} f(x_j) w_{kj}^{o} + b_k^{o} \quad (3c)$$

Where x_j = the net input to the node j in the hidden layer, y_i = the input to a neuron, w_{ji}^{in} = the weight associated with each input connection from i_{th} to j_{th} neuron in the hidden layer, b_j^{in} = the bias of the jth neuron in the hidden layer, y_k = the net input to the node k in the output layer, w_{kj}^{o} = the weight linking neuron in the hidden layer from jth to kth neuron in the output layer, and b_k^{o} = the bias of the kth neuron in the output layer. p = the number of neurons in the input layer, q = the number of neurons in the hidden layer, and k = the number of neurons in the output layer.

Meta-heuristics optimisation algorithm

Meta-heuristics optimisation algorithms are largely inspired, and stimulated by the social behaviour of nature as they mimic the dynamic movements, and communications of some creatures such as insects, fishes, and birds (Nassef et al., 2018). The algorithms outperform other optimisation tools such as gradient-based and derivative-free algorithms. Other examples of meta-heuristics algorithms are Hill Climbing, Trust Region Technique, Simulated Annealing, Differential Evolution, PSO, GA, and FA (Yang, 2011). Due to their wide applications and accuracy over other meta-heuristics algorithms, PSO, GA, and FA were utilised in this work (Doroody & Kiong, 2018).

Particle swarm optimisation (PSO)

The PSO is one of the algorithms that mimic the social behaviour of fish and birds which was initially developed by James Kennedy and Russell C Eberhart in 1995 as an optimisation tool (Nassef et al., 2018). It is a swarm intelligence with a population size (P) of a candidate solution called a particle. Each population has its position X_j^m, velocity V_j^m, personal, and global best (Pb_j^m and Gb_j^m). The particles constitute a swarm, adjust their "flying" direction, and position based on their own best experience, and move within the search space to locate the best solution (Rezk et al., 2017). According to the authors, each particle keeps tracking its best position, personal best (pbest), and best value that has the global best (gBest). Therefore, to provide the optimum solution(s) to the optimisation problem, the particles communicate and learn from one another using the particle's

position update rules as shown in Equation 4(a and b) (Mohamed et al., 2018).

$$p(k+1 = p(k) + v(k+1) \quad (4a)$$

$$v(k+1) = w * v(k) + c_1 * r_1 * (pBest - p) + c_2 * c_2 * (gBest - p) \quad (4b)$$

where p is the particle's current position; v is the particle's velocity; c_1 and c_2 are the weight of local information and the weight of global information, respectively; pBest and gBest are the best position of the particle and the best position of the swarm found so far, respectively; r_1 and r_2 are two random variables generated in the band of [0 1]. Note that Equation 4a is for updated particle velocity while 4b is for updated particle position as shown in Figure 1.

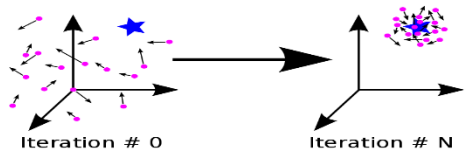

Figure 1: Particle description in social space

Therefore, PSO is used to find the optimal variables; MeOH: oil molar ratio, reaction time, reaction temperature, and catalyst quantity that maximises the percentage yield of biodiesel from WRF using the AKC-CEC catalyst. Thus, the cost function given in Equation 4c was employed:

$$f(x) = -(R_p) \quad (4c)$$

where Rp is the %yield of biodiesel, the negative sign is to convert the maximisation problem into a minimisation problem, and x is the controlling parameters' vector. Please note that Rp here is not the same as Y(x) in equation 2. Y(x) gives us the relationship between the input parameters such as time, temperature, etc., and biodiesel yield but no information on the maximum biodiesel yield that can be obtained at minimal input parameter values, and this is where Rp comes into play. Where Rp can be mean square error, root mean square error, etc. of Y(x) actual to Y(x) estimated

The PSO algorithm was applied to investigate with 40 particles (solutions) and 1000 iterations as shown in Table 3. The table also includes the self and social information parameters such as acceleration elements a_1 and a_2, inertia weight ω, Varmin (lower bound of unknown variables), and Varmax (upper bound of unknown variables) maximum generation T.

Table 3: PSO algorithm-centric parameters

Parameter	Value
Crossover	1
Y	0.1
Mutation	0.01
Varmin	-10
Varmax	10
Npop	40
T	1000

Genetic algorithm (GA)

The GA is a meta-heuristics optimisation method developed by David E. Goldberg based on the analogy of biological processes. The GA is influenced by Darwin's theory of evolution which claims that an organism's survival is determined by the rule "the strongest species survives." The theory proposed that an organism's survival may be by reproduction, crossover, and mutation. A chromosome is a collection of genes that could be generated by a GA having its value as numerical, binary, symbols, or characters, depending on the problem to be solved. When running this optimisation tool, some chromosomes marry, giving birth to new sets of chromosomes, and a few of them also experience gene(s) mutation. The number of chromosomes that would crossover and mutate is determined by the mutation and crossover parameters of the GA. For the next cycle, the chromosome with the highest fitness value would be chosen and converge to a particular value after numerous rounds, which is the optimal answer for the stated problem. It is noteworthy that the GA exhibits extensive applicability in this endeavour. It is an exceedingly valuable tool for validating the accuracy of the forecasted model (Kolakoti et al., 2020). Figure 2 depicts the process associated with utilising GA to solve optimisation problems using an assembly of chromosomes referred to as a population. The model equation generated by the RSM was employed to evaluate the GA optimisation approach for the optimum biodiesel yield. The MATLAB version 2021 was used to analyse the RSM model for optimisation through the GA (Dewangan et al., 2023). This was investigated by developing a MATLAB code that represents the RSM model (Eq. 2) and GA with the constraints/set of parameters in Table 4, to obtain the optimum result.

Table 4: Genetic algorithm parameters

Parameters	Value
a_1	2
a_2	2
ω	1
Varmin	-10
Varmax	10
Nparticles	40
Iterations	1000

Firefly algorithm (FA)

The FA has been identified as a relatively easy and simple algorithm for solving various optimisation problems effectively (Doroody & Kiong, 2018). It is also one of the most effective meta-heuristic algorithms that rely on the flashing behaviour of fireflies based on three different characteristics (Fajuke & Raji, 2022; Yang, 2011). Researchers have identified certain characteristics of fireflies. Firstly, it has been observed that fireflies are all unisex in terms of gender (Fajuke & Raji, 2022). Secondly, the intensity of flashing displayed by fireflies could have an impact on their behaviour (Dirik, 2023).

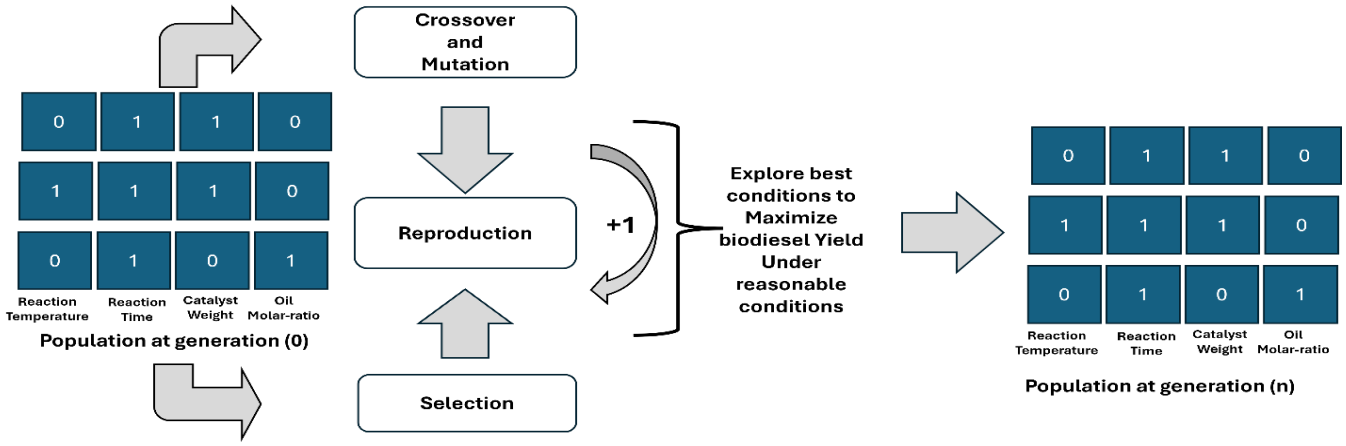

Figure 2: Description of genetic algorithm

Finally, the brightness of fireflies can be influenced by the objective function, which is contingent upon the kind of optimisation problem being addressed, whether it is a minimum or maximum (Altherwi, 2020; Fajuke & Raji, 2022).

The objective of this study was to solve the maximisation problem, and the goal function is therefore proportional to the firefly's brightness. The FA's primary parameters are light intensity (I), attractiveness (β), and light absorption coefficient (γ). The light intensity (I) can thus be expressed as in Equation 5a:

$$I = I_o e^{-\gamma r} \quad (5a)$$

Where r = distance between fireflies, I_o = light intensity at distance (r = 0). The attractiveness of fireflies is expressed in Equation 5b as given in the literature (Altherwi, 2020).

$$\beta = \beta_o e^{-\gamma r^2} \quad (5b)$$

Where β_o = attractiveness of a firefly at distance (r = 0). If a firefly (i) has less brightness, the movement towards the brighter firefly (j) can be evaluated using Equation 5c (Watanabe et al., 2022):

$$X_i = X_i + \beta_o e^{-\gamma r_{ij}^2}(X_j - X_i) + \alpha * \varepsilon_i \quad (5c)$$

Where X_i = a less bright firefly, and X_j = a bright firefly. Therefore, the FA control parameters of β_o, $\propto$, γ, T (total number of iterations to run), N (number of fireflies), $Xmin\ and\ Xmax$ (minimum and maximum range foisted on the five $b\ to\ f$ values) are listed in Table 5.

Table 5: Firefly algorithm parameters

Parameter	Value
α	2
β	2
γ	1
X_{min}	-10
X_{max}	10
N	40
T	1000

When these different models have been developed based on the different algorithms (the equations/models are named after the algorithm used to determine the fitting parameters). The models are then optimised through a grid search without altering the model fitting parameters, the grid search essentially involves fixing the fitting parameters while the features (MeOH-to-oil mole ratio, reaction time, temperature, and catalyst quantity) are varied. Grid search is chosen because it is generally a cheaper method based on computational cost compared to the optimisation algorithms (PSO, GA, and FA) used for mapping the biodiesel yield to the features.

Workflow for the maximization of biodiesel yield and minimization of operating conditions

The workflow consists of three main steps:

1. **Model Development**: Using RSM, ANN, FA, GA, and PSO to derive fitting parameters a,b,c,… and construct a predictive model. In this case, the optimization algorithm is used for determining the mathematical expression fitting parameters by minimising the objective function. The models/mathematical expressions obtained by the models are named by the name of the algorithm used to obtain the fitting parameters or target and feature mapping.
2. **Optimisation**: Identifying the optimal reaction conditions—such as time, temperature, and catalyst quantity—to maximise biodiesel yield. For this section, grid search optimisation was done to determine the minimal experimental conditions required to maximise biodiesel yield by using the models/mathematical expressions obtained from Step 1(The fitting parameters are fixed while the features are varied, so the model/mathematical expression gotten does not change in any way).
3. **Validation:** Experimentally synthesising biodiesel under optimised conditions to verify the alignment between computational predictions and real-world outcomes.

Problem Setup:

1. First Objective: Minimise the error between the predicted biodiesel yield Y (from the equation) and the actual biodiesel yield (Y_{data}). Where X_1, X_2, X_3, and X_4 represent alcohol molar ratio, time, temperature, and catalyst quantity.

$$Minimise: Error = \sum_{i=1}^{n} \left(Y_{data,i} - \left(aX_{1,i} + bX_{2,i} + cX_{3,i} + dX_{4,i}\right)\right)^2$$

2. Second Objective: Maximise Y_Y by optimising X_1, X_2, X_3, and X_4 with fixed coefficients a, b, c, and d: Maximise: $Y = aX_1 + bX_2 + cX_3 + dX_4$

Unified Representation which is the Desirability of the Multi-objective optimisation would be defined as; We represent this as a single optimisation problem by introducing weights α and β to balance the two objectives. The combined objective becomes:

Optimise:

$$\mathcal{L} = \alpha \sum_{i=1}^{n} \left(Y_{data,i} - \left(aX_{1,i} + bX_{2,i} + cX_{3,i} + dX_{4,i}\right)\right)^2 - \beta(aX_1 + bX_2 + cX_3 + dX_4)$$

Explanation:

1. The first term $\alpha \sum_{i=1}^{n} \left(Y_{data,i} - \left(aX_{1,i} + bX_{2,i} + cX_{3,i} + dX_{4,i}\right)\right)^2$ minimises the error between predicted and actual Y, where α controls the weight of this objective.
2. The second term $-\beta(aX_1 + bX_2 + cX_3 + dX_4)$ Maximizes Y by optimising X_1, X_2, X_3, and X_4 with β controlling the weight of this objective.

Constraints:

- Constraints with the following ranges for X_1, X_2, X_3, and X_4 are used for the grid search in the second optimisation are; (min, max); (9, 12), (1, 4), (80, 95), and (2, 7). While Y is limited between 0 and 1.
- a, b, c, d are fixed during the second optimisation phase. This formulation provides a single equation that balances both objectives, where you can tune α and β to prioritise one objective over the other. Note that the representations here are the basic form of the optimisations carried out in this study.

C. Evaluation of Models Predictability

The RSM, ANN, PSO, GA, and FA models evaluated for the prediction of the optimum biodiesel yield were appraised statistically using mean squared error (MSE), root mean squared error (RMSE), coefficient of determination (R^2), and absolute average deviation (AAD). The objective was to analyse the output error between the actual and predicted values to evaluate the predictability, precision, and accuracy, and predictability of each model. Meanwhile, the R^2 value is usually a reflection of the degree of fitness of the model, as the closer it is to unity the better the model fits the experimental data (Betiku & Taiwo, 2015). The AAD is another important index to analyse the model output error between the actual and the predicted data which must be to the minimum possible (Betiku & Ajala, 2014). Consequently, Equations 6(a – d) are the mathematical expressions for estimating the values of MSE, RMSE, R^2, and ADD, respectively:

$$\mathrm{MSE} = \frac{1}{n}\sum_{i=1}^{n}(y_i - y_{di})^2 \quad (6a)$$

$$RMSE = \sqrt{MSE} \quad (6b)$$

$$R^2 = 1 - \sum_{i=1}^{n}\left(\frac{(y_i - y_{di})^2}{(y_{di} - y_m)^2}\right) \quad (6c)$$

$$ADD = \left\{\left[\sum_{i=1}^{n}(|y_i - y_{di}|/y_{di})\right]/n\right\} X\ 100 \quad (6d)$$

where n is the number of points, y_i is the predicted value obtained from the model, y_{di} is the actual value, and y_m is the average of the actual values.

Therefore, the model with minimum RMSE, AAD and maximum R^2 is taken as the best, in addition to the residual values between the actual and predicted data (Betiku & Taiwo, 2015).

D. Fuel Properties of the Biodiesel from WRF

The gas chromatography (GC-MS) analysis was also performed, to determine the quality and quantity of the Fatty Acid Methyl Ester (FAME) in the biodiesel. The procedure and operating conditions employed for the GC-MS analysis have been reported in the literature (Ajala et al., 2020).

III. RESULTS AND DISCUSSION

A. Optimisation studies of biodiesel production from WRF

RSM by I-optimal experimental design

Empirical data were collected from the transesterification of WRF for biodiesel production in the presence of AKC-CEC catalyst using RSM by I-optimal experimental design as shown in Table 7. The process conditions considered for the optimisation are also presented in the experimental matrix as shown in the table. The empirical matrix exhibiting the greatest biodiesel yield of 81% is associated with experimental run 25 as indicated in the table. This includes MeOH: oil molar ratio of 18:1, reaction time of 4 h, reaction temperature of 70°C, and catalyst quantity of 15% (w/w).

Table 8 shows the ANOVA for the biodiesel yield data with an F-value of 27.58 which implies the significance of the model. The *p*-value for the model also indicates that there is only a 0.02% chance that an F-value this large could occur due to noise. Based on a *p*-value of <0.0500, the model terms of B, C, D, AB, AD, CD, A^2, B^2, D^2, ABC, ACD, BCD, A^2B, AB^2, AC^2, B^2C, B^2D, BD^2, C^2D, CD^2, B^3, and D^3 are significant.

Table 7: Empirical data for biodiesel yield using RSM by I-optimal experimental design

Exp. Run	A: MeOH: oil molar ratio (w/w)	B: Reaction time (h)	C: Reaction temperature (°C)	D: Catalyst quantity (w/w)	% Biodiesel Yield
1	16.80	2.00	90.00	5.00	53.16
2	13.92	2.00	78.00	5.65	36.86
3	12.00	4.00	90.00	5.00	40.65
4	12.12	2.40	75.00	12.25	35.75
5	17.82	2.94	70.00	12.60	34.71
6	18.00	2.00	70.00	5.00	71.71
7	17.40	3.50	85.70	14.90	80.26
8	14.40	3.01	81.30	9.50	64.35
9	16.68	3.57	90.00	9.50	80.33
10	12.60	3.32	70.7.0	8.20	17.26
11	18.00	4.00	70.00	7.00	62.61
12	18.00	2.53	84.80	7.85	53.74
13	18.00	2.00	90.00	14.80	39.23
14	15.00	2.56	90.00	14.85	21.06
15	13.86	4.00	90.00	15.00	39.65
16	17.04	2.27	77.40	15.00	66.18
17	15.27	2.53	70.00	5.50	60.17
18	12.00	2.86	82.20	5.15	63.74
19	17.10	2.66	85.10	12.47	70.26
20	18.00	4.00	90.00	5.00	78.71
21	12.21	3.28	87.80	12.80	41.92
22	13.68	3.46	76.59	15.00	46.36
23	12.54	2.21	90.00	8.20	68.45
24	13.68	3.46	76.59	15.00	47.81
25	18.00	4.00	70.00	15.00	81.00
26	12.00	4.00	70.00	15.00	36.82
27	17.25	3.40	76.30	5.35	44.19
28	17.25	3.40	76.30	5.35	42.49
29	12.42	4.00	79.70	9.70	26.81
30	18.00	4.00	78.00	11.70	74.37
31	14.22	3.20	89.30	5.00	74.59
32	15.57	4.00	84.76	6.50	60.19
33	16.50	2.00	72.00	8.90	48.39
34	12.00	2.00	70.00	5.00	36.89
35	13.59	2.00	70.00	15.00	45.04
36	15.27	3.92	70.50	12.55	50.59
37	12.12	2.40	75.00	12.25	61.00
38	14.68	2.80	70.00	11.45	66.04
39	14.88	2.01	85.10	12.25	64.55
40	12.99	4.00	72.00	5.00	76.66

Table 8: ANOVA and fit statistical data for biodiesel yield

Source	Sum of Squares	df	Mean Square	F-value	*p*-value	
Model	12875.03	34	378.68	27.58	0.0002	significant
A-MeOH: oil molar ratio (w/w)	9.20	1	9.20	0.6698	0.4444	
B-Reaction time (h)	242.82	1	242.82	17.69	0.0056	
C-Reaction temperature (^oC)	1069.43	1	1069.43	77.90	0.0001	
D-Catalyst quantity (w/w)	448.96	1	448.96	32.70	0.0012	
AB	702.09	1	702.09	51.14	0.0004	
AC	69.45	1	69.45	5.06	0.0655	
AD	1037.65	1	1037.65	75.59	0.0001	
BC	61.54	1	61.54	4.48	0.0786	
BD	13.35	1	13.35	0.9724	0.3622	
CD	88.85	1	88.85	6.47	0.0438	
A^2	84.75	1	84.75	6.17	0.0475	
B^2	248.43	1	248.43	18.10	0.0054	
C^2	8.75	1	8.75	0.6376	0.4550	
D^2	99.99	1	99.99	7.28	0.0356	
ABC	502.31	1	502.31	36.59	0.0009	
ABD	47.07	1	47.07	3.43	0.1135	
ACD	408.67	1	408.67	29.77	0.0016	
BCD	811.08	1	811.08	59.08	0.0003	
A^2B	189.17	1	189.17	13.78	0.0099	
A^2C	21.28	1	21.28	1.55	0.2595	
A^2D	68.17	1	68.17	4.97	0.0674	
AB^2	336.64	1	336.64	24.52	0.0026	
AC^2	176.21	1	176.21	12.84	0.0116	
	1.94	1	1.94	0.1416	0.7196	
B^2C	212.51	1	212.51	15.48	0.0077	
B^2D	204.97	1	204.97	14.93	0.0083	
BC^2	46.52	1	46.52	3.39	0.1152	
BD^2	508.16	1	508.16	37.02	0.0009	
C^2D	1106.32	1	1106.32	80.59	0.0001	
CD^2	1166.44	1	1166.44	84.97	< 0.0001	
A^3	15.17	1	15.17	1.10	0.3337	
B^3	187.48	1	187.48	13.66	0.0101	
C^3	66.09	1	66.09	4.81	0.0707	
D^3	467.67	1	467.67	34.07	0.0011	
Residual	82.37	6	13.73			
Lack of Fit	59.71	3	19.90	2.64	0.2236	not significant
Pure Error	22.66	3	7.55			
Cor Total	12957.40	40				

R^2 = 0.9936 **Adjusted R^2** = 0.9576 **Adeq Precision** = 20.1474

Std. Dev = 3.71 Mean = 52.28 **C.V. %** = 7.09

Therefore, all these model terms in terms of their process conditions were effective in biodiesel production (Ardabili et al., 2018). Furthermore, the "Lack of Fit F-value" of 2.64 implies that the Lack of Fit is not significant relative to the pure error. There was a 22.36% chance that a Lack of Fit F-value this large could occur due to noise. The non-significant lack of fit is good, as the model is desired to fit. The correlation coefficient (R^2) value of 0.9936 obtained from the analysis is shown in Table 5. The R^2 value is very close to unity which indicates that the model is a perfect fit for the experimental data (Ajala et al., 2019). Also, the adjusted R^2 of 0.9576 obtained depicted a reasonable agreement with the R^2 value. The low coefficient of variation (C.V) of 7.09% further established that the fitted model is reliable.

The 3D surface plots shown in Figure 3 further describe the combined effect of any two process conditions on the biodiesel yield. Figure 3a shows that the biodiesel yield increases from 67% to 83% as the MeOH: oil molar ratio decreases from 18:1 to 12:1 (w/w) and reaction time increases from 2 h to 2 h 30 mins. The excess MeOH in the reaction could increase the solubility of glycerol and drive the equilibrium back to the left, thereby lowering the biodiesel yield. It could also inactivate the catalyst, promote the backward reaction of the process, lower biodiesel yield, and promote soap formation (Erchamo et al., 2021; Ngige et al., 2023). In addition, it has been reported by the authors that extending the reaction time beyond the optimum level could potentially result in a decrease in biodiesel yield, as a consequence of the reversible reaction. The extended reaction time beyond 2 h 30 mins observed in this study may lead to the hydrolysis of esters, consequently generating additional fatty acids. This, in turn, promotes the formation of soap and subsequently diminishes the overall yield of biodiesel.

Figure 3b depicts that the biodiesel yield increases from 52% to 83% as the MeOH: oil molar ratio decreases from 18:1 to 12:1 (w/w) and reaction temperature increases from 70^{o}C to 90^{o}C. This shows that the interaction between MeOH: oil molar ratio at 12:1 (w/w) and temperature at 90^{o}C gave the optimum biodiesel yield of 83%. This showed that the higher temperature of 90^{o}C caused a faster molecular movement/kinetic energy of MeOH and oil when it was at a ratio of 12:1 (w/w). This resulted in an increased collision between the reactant of MeOH and oil and produced the heat that converted WRF to biodiesel (Moulita et al., 2019). Therefore, a higher temperature of 90^{o}C increased the reaction rate due to increasing kinetic energy and gave a higher biodiesel yield of 83%. Figure 3c shows the combined effect of MeOH: oil molar ratio (w/w) and catalyst quantity (%, w/w) on biodiesel yield. The figure revealed that as the MeOH: oil molar ratio decreases from 18:1 to 12:1 (w/w) with a decrease in catalyst quantity from 15 to 5% (w/w), the biodiesel yield increases from 54.6% to 83%. On the other hand, increased catalyst quantity is supposed to facilitate the provision of a more active site for the reaction. This, in turn, could lead to an enhanced adsorption process aimed at breaking the OH bond in MeOH. Hence, the MeOH is broken down into methoxide ions and hydrogen cations while the methoxide ions in the catalyst react with triglyceride molecules to form biodiesel (Buchori et al., 2020). However, the excessive quantity of catalyst (> 5%, w/w) in this study resulted in the formation of slurry with a reactant mixture, thereby inhibiting and subsequently lowering the yield of biodiesel (Buchori et al., 2019). Figure 3d depicts the effect of the interaction between reaction time (h) and reaction temperature (^{o}C) on biodiesel yield. The figure showed that as the reaction time increases from 2 h to 2 h 30 mins and temperature increases from 70^{o}C to 90^{o}C, the biodiesel yield increases from 61.8% to 83%. The biodiesel yield decreased to 51.2% after a reaction time of 2 h 30 mins. This decline could be attributed to the evaporation of MeOH at the elevated temperature during the prolonged reaction time (Daniyan et al., 2015). Also, the decrease in the biodiesel yield when the reaction time was beyond 2 h 30 mins at 90^{o}C may be due to the reversible nature of the reaction. Figure 7e shows the combined effect of reaction time (h) and catalyst quantity (%, w/w) on biodiesel yield. The figure revealed that the higher reaction time beyond 2 h 30 mins and catalyst quantity of >5% (w/w) decreases the biodiesel yield to 16.6%. The prolonged reaction time when a higher catalyst quantity was used for the reaction could result in soap formation instead of biodiesel. This is because the excess quantity of the catalyst could have boosted the viscosity of the reaction mixture and lowered the effective mass transfer between the catalyst and reactants, thus, reducing the biodiesel yield (Ajala et al., 2024).

Figure 3f shows the interactive effect of reaction temperature (^{o}C) and catalyst quantity (%, w/w) on the biodiesel yield. It was also observed from the figure that the reaction temperature of 90^{o}C, and catalyst quantity of 5% (w/w) gave the maximum biodiesel yield of 83%. This corroborates the claim in the literature that a higher temperature accelerates the rate of reaction, thus, shifting the reaction equilibrium forward (Ajala et al., 2024). The higher temperature of the reaction also increases the reactant activation, higher oil miscibility, and lowers the viscosity of reactants, to produce a higher yield of biodiesel. At a higher temperature when excess catalyst quantity is in use, the biodiesel yield is thus decreased as the operating conditions promote the formation of glycerol (Ngige et al., 2023).

Furthermore, regression analysis was performed on the experimental data that describe the biodiesel production from WRF, to obtain a model equation in terms of the coded factors as shown in Equation 7.

$$\text{Biodiesel Yield (\%)} = 54.00207 + 0.761033*A - 13.3561*B + 27.8959*C + 19.94765*D + 8.689123*A*B + 2.595758*A*C + 10.10684*A*D + 1.836874*B*C + 1.590911*B*D - 3.27039*C*D - 7.70069*A*A^2 + 4.482226*B*A^2 + 0.772769*C*A^2 + 2.950177*D*A^2 + 8.628396*A*B*C + 2.450348*A*B*D + 8.001729*A*C*D + 9.185553*B*C*D - 7.01563*A*A^2*B + 5.647359*A*A^2*C + 3.671024*A*A^2*D + 14.61669*A*B*A^2 + 6.362699*A*C*A^2 - 0.52451*A*D*A^2 - 6.52097*B*A^2*C + 6.753357*B*A^2*D + 3.126468*B*C*A^2 + 14.1587*B*D*A^2 - 18.1711*C*A^2*D - 20.8797*C*D*A^2 - 1.03583* A*A^3 + 13.00634*B*A^3 - 13.3148*C*A^3 - 21.1721* D*A^3 \quad (7)$$

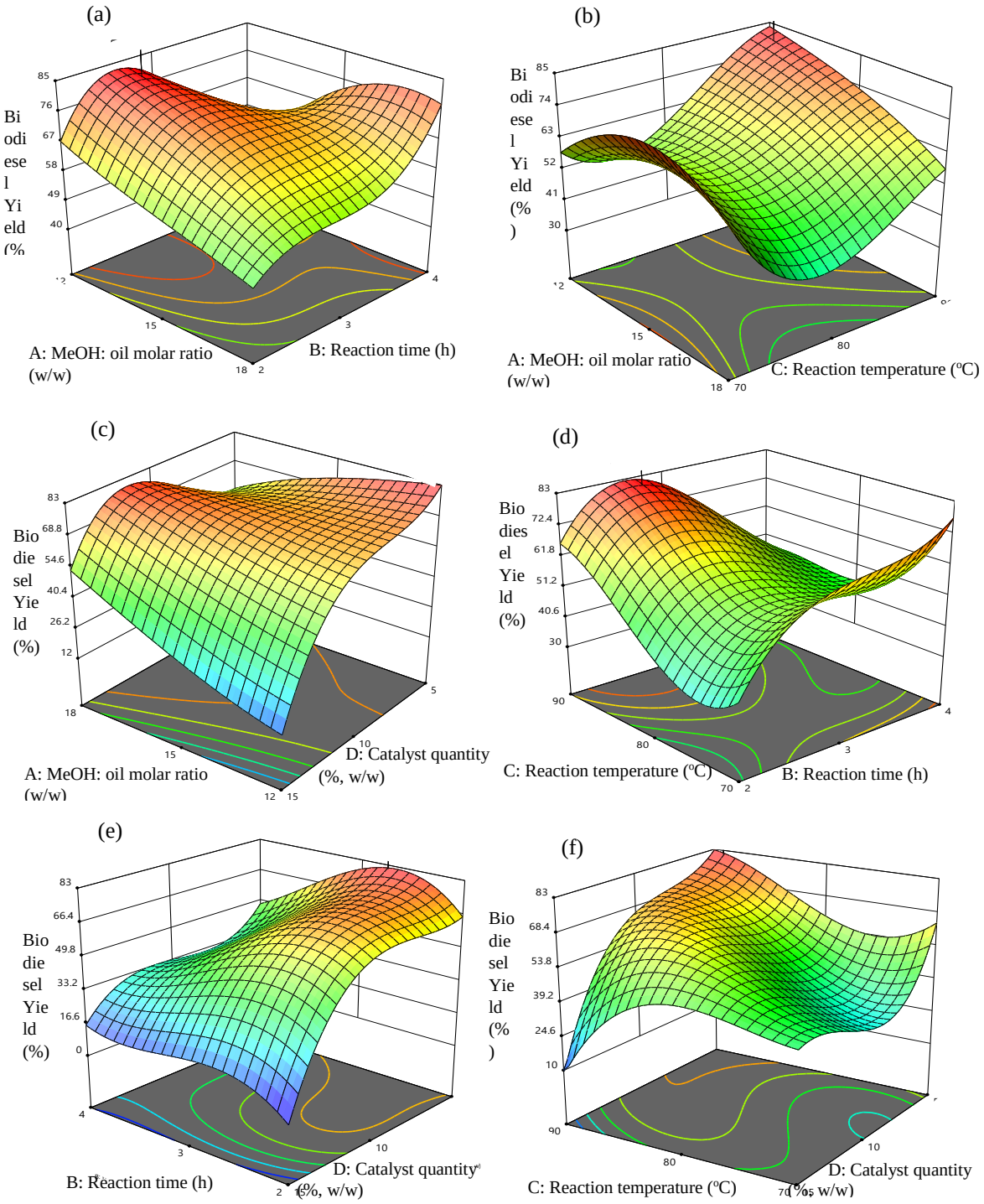

Figure 3: 3D plots for the effects of (a) MeOH: oil molar ratio and reaction time, (b) MeOH: oil molar ratio and reaction temperature, (c) MeOH: oil molar ratio and reaction and catalyst quantity, (d) Reaction time and reaction temperature, (e) Reaction time and catalyst quantity, and (f) Reaction temperature and catalyst quantity on biodiesel yield reaction and catalyst quantity

The numbers in this equation are the fitting parameters that go through the algorithm. Solving the equation gave an optimum biodiesel yield of 82.75% at optimal process conditions of

MeOH: oil molar ratio of 12.07 (w/w), reaction time of 2.58 h, reaction temperature of 89.60ºC, and catalyst quantity of 5.06% (w/w) as shown in Table 9.

Table 9: Optimum biodiesel yield and the corresponding optimal process conditions

Response	Process conditions			
Biodiesel Yield (%)	MeOH: oil molar ratio (w/w)	Reaction time (h)	Reaction temperature (ºC)	Catalyst quantity (%, w/w)
82.75	12.07	2.58	89.60	5.06

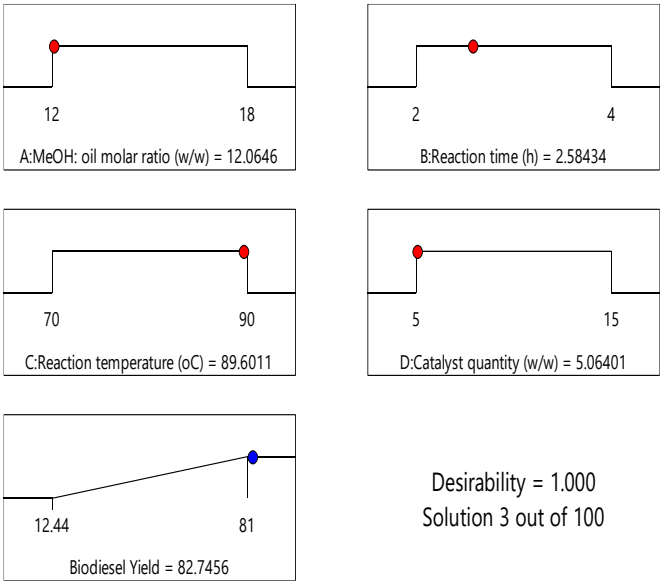

Figure 4: Ramp plots for the process conditions and biodiesel yield

These data were obtained after the optimisation analysis of the equation using Design Expert Software Version 11.0. The ramp plot shown in Figure 4 confirms that the optimal solutions fall within the experimental boundaries. Therefore, it can be concluded that the I-optimal RSM embedded in the design expert successfully optimised the conversion of WRF to biodiesel using an AKC-CEC catalyst.

Artificial neural network (ANN)

A multilayer feedforward with an incremental back propagation network and Tanh as a transfer function was considered for the ANN model as shown in Figure 5. The figure shows that the model comprised a hidden layer, and an output layer.

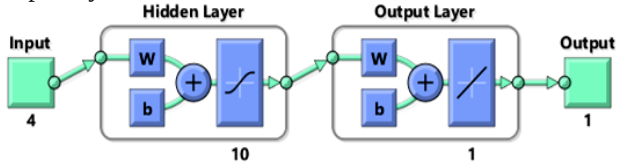

Figure 5: Number of layers in the neural network

Figure 6a shows the plots of ANN regression for training, validation, test, and overall, as well as their high regression values (R close to 1). As shown in the figure, the R^2 value for the training data set was 0.97989. At the same time, those of validating, and testing data sets were evaluated as 0.81162, and 0.76239, respectively. The R^2-value for all the data sets was obtained as 0.81495 as shown in Figure 6a. Figure 6b shows the best validation performance of 105.0589 at epoch for Mean square error (MSE) analysis of the biodiesel yield. This showed the ability of generalisation of the unknown data which implies that the empirical model could derive from the ANN model. Furthermore, the high R^2 obtained demonstrates a strong connection between predicted and experimental data, indicating a good fit between them as shown in Figure 7a. It could be deduced that the experimental and predicted values in training, validating, and testing data sets showed the capability of ANN to predict the known data responses. The residual plot shown in Figure 7b demonstrates a good distribution of errors for the equation with a maximum deviation of +/-30. Figure 7c shows the plot of error analysis (mean squared error) for the biodiesel yield. Thus, the overall model's performance satisfactorily predicts biodiesel yield with a high level of accuracy.

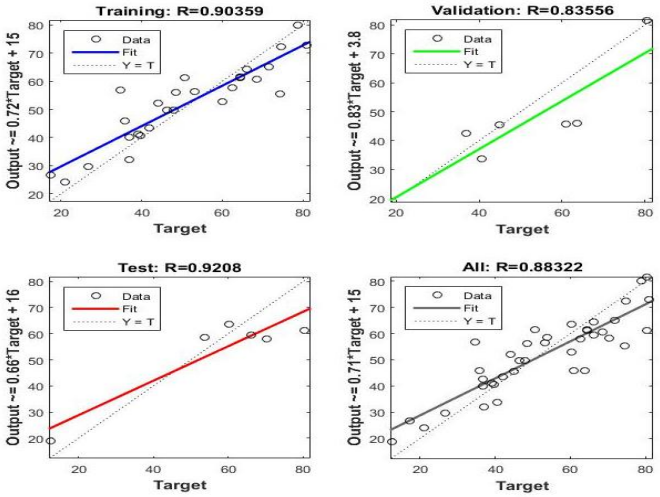

Figure 6a: Regression plots for the ANN model

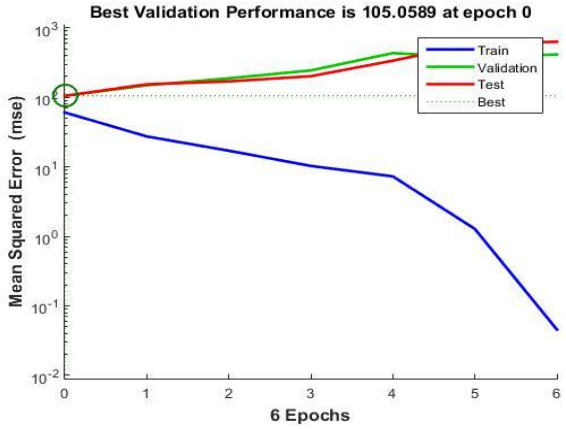

Figure 6b: ANN's best performance in terms of MSE at different Epochs

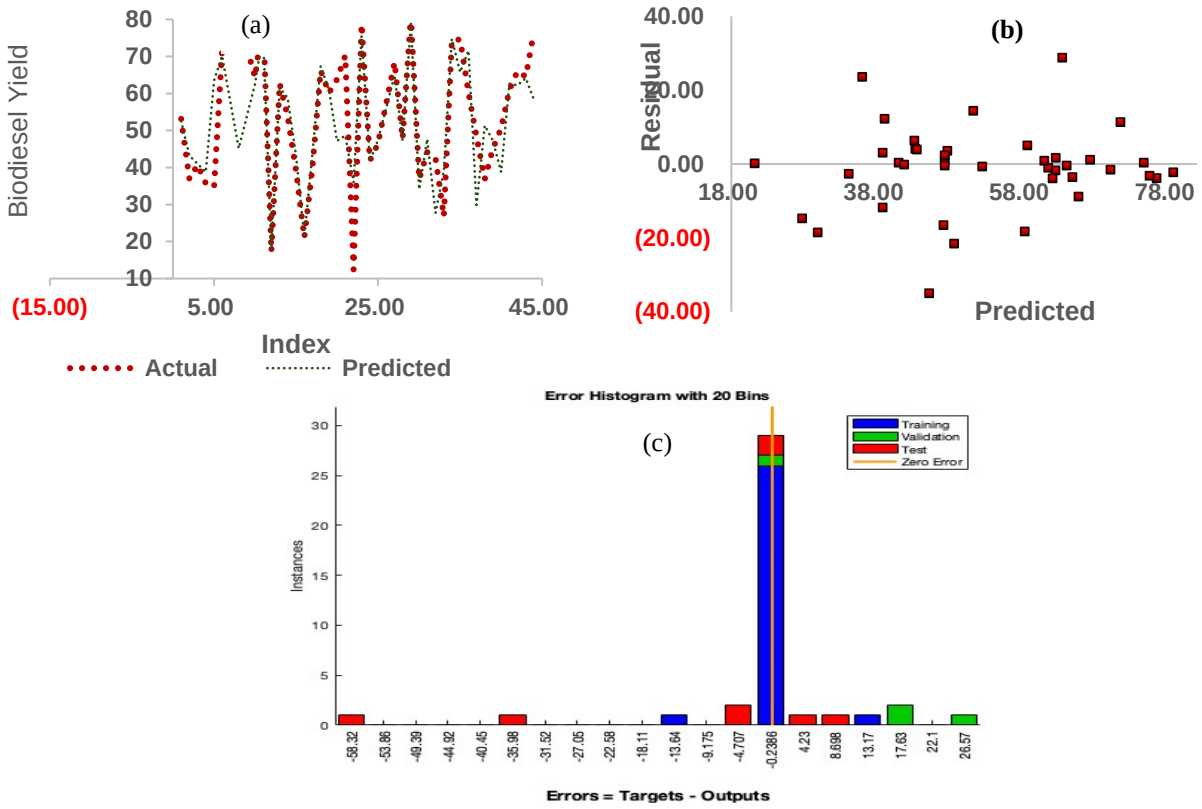

Figure 7: ANN plot of biodiesel yield for (a) actual and predicted data, (b) residual, (c) error plot

B. Meta-heuristics Algorithms for Biodiesel Yield Optimisation

PSO biodiesel model

The objective was to find the optimal values for MeOH: oil molar ratio, reaction time, reaction temperature, and catalyst quantity that would produce maximum biodiesel yield. From the iterations of the algorithm, the %yield of biodiesel obtained for the PSO, and its residual are also presented in Table 10. The residual column shows that the PSO results of biodiesel yield differ in some instances from those of the RSM. This could mean an improvement in the optimisation process.

Based on the experimental data shown in Table 1, the lower and upper limits of the four choice variables are [12, 2, 70, 5] and [18, 4, 90, 15], respectively. The objective function shown in Equation 4c was transformed into Equation 8 through the PSO algorithm, with the decision variables as the constraints for the analysis.

Biodiesel Yield (Y, %) = 53.645*A + 1000*B - 21.8365*C - 170.996*D - 41.7691*A*B - 0.811578*A*C - 4.36003*A*D - 2.68746*B*C - 30.9019*B*D + 4.25821*C*D + 4.26718*A^2 - 154.712*B^2 + 0.100304*C^2 + 8.00336*D^2 + 0.258824*A*B*C + 0.278133*A*B*D + 0.0479247*A*C*D + 0.146772*B*C*D - 0.531524*A^2*B - 0.013234*A^2*C - 0.010964*A^2*D + 6.11122*B^2*A + 0.000727168*C^2*A + 0.0387787*D^2*A - 0.782108*B^2*C + 0.649904*B^2*D + 0.0139687*B*C^2 + 0.560553*B*D^2 - 0.024915*C^2*D - 0.074711*C*D^2 - 0.0549138*A^3 + 13.1844*B^3) + 0.000567099*C^3 - 0.143144*D^3 (8)

The numbers in this equation are the fitting parameters that go through the algorithm.

Figure 8a shows the plots of the observed and predicted values obtained from the PSO against the empirical run. The figure revealed that the predicted data was a close match to the actual data for the biodiesel yield. This is because there was an overlap in most cases of the curve line, even though there were few veers off of the RSM curve line, as shown in the figure. Figure 8b depicts the regression plot of the PSO model which revealed about 85% prediction accuracy. The residual plot shows a good distribution of errors for the equation with a maximum deviation of +/-20 as shown in Figure 8c. The figure showed that the errors are well dispersed which indicates that the model performance is good. The findings from the PSO analysis suggest that the obtained result is stable. Evidently from the figure, the data showed high repeatability (Yousef et al., 2020). This result demonstrates the PSO model's robustness for optimisation and the rate constants' convergence, reflecting a perfect agreement between the predicted and experimental results (Kadi et al., 2019).

Table 10: Comparative analysis of biodiesel yield prediction for the models

	MODELS' PREDICTION FOR BIODIESEL YIELD								
	RSM	ANN		PSO		GA		FA	
Exp. Run	Yield	Yield	Residual	Yield	Residual	Yield	Residual	Yield	Residual
1	53.16	52.50	(0.66)	52.96	(0.20)	55.52	2.36	51.80	(1.36)
2	36.86	43.17	6.31	37.17	0.31	39.86	3.00	36.17	(0.69)
3	40.65	41.03	0.38	42.38	1.73	52.78	12.13	42.24	1.59
4	35.75	38.83	3.08	54.84	19.08	56.31	20.56	54.10	18.35
5	34.71	63.52	28.80	42.27	7.56	44.97	10.26	41.02	6.31
6	71.71	70.17	(1.54)	69.63	(2.08)	72.08	0.37	68.15	(3.56)
7	80.26	45.22	(35.04)	76.77	(3.49)	79.49	(0.77)	75.96	(4.30)
8	64.35	62.60	(1.75)	57.89	(6.46)	62.34	(2.01)	57.13	(7.22)
9	80.33	76.50	(3.83)	79.22	(1.11)	85.49	5.16	78.53	(1.80)
10	17.26	17.83	0.57	39.25	21.99	45.73	28.47	38.56	21.30
11	62.61	61.56	(1.05)	58.49	(4.12)	67.81	5.20	57.37	(5.24)
12	53.74	58.74	5.00	52.65	(1.09)	55.75	2.01	51.46	(2.29)
13	39.23	43.32	4.09	38.93	(0.30)	36.35	(2.89)	37.69	(1.54)
14	21.06	21.23	0.17	41.64	20.58	40.96	19.90	40.86	19.80
15	39.65	43.52	3.87	38.98	(0.67)	44.00	4.35	38.77	(0.88)
16	66.18	67.34	1.16	63.54	(2.64)	62.38	(3.80)	62.32	(3.86)
17	60.17	61.05	0.88	61.84	1.67	66.01	5.84	60.72	0.55
18	63.74	47.18	(16.56)	60.34	(3.40)	65.99	2.25	59.77	(3.97)
19	70.26	48.66	(21.60)	73.17	2.91	74.46	4.20	72.12	1.86
20	78.71	75.52	(3.19)	78.18	(0.53)	87.97	9.26	77.44	(1.27)
21	41.92	41.76	(0.16)	42.14	0.22	45.84	3.92	41.80	(0.12)
22	46.36	47.37	1.01	49.28	2.92	52.67	6.31	48.68	2.32
23	68.45	64.90	(3.55)	70.93	2.48	73.41	4.96	70.26	1.81
24	47.81	47.37	(0.44)	49.28	1.47	52.67	4.86	48.68	0.87
25	81.00	78.79	(2.21)	80.19	(0.81)	85.96	4.96	79.16	(1.84)
26	36.82	34.16	(2.66)	33.08	(3.74)	39.45	2.63	32.66	(4.17)
27	44.19	47.71	3.52	47.63	3.44	54.73	10.54	46.56	2.37
28	42.49	27.75	(14.74)	47.63	5.14	54.73	12.24	46.56	4.07
29	26.81	39.08	12.27	24.75	(2.06)	33.51	6.70	24.39	(2.42)
30	74.37	74.72	0.35	76.87	2.50	84.15	9.78	75.95	1.58
31	74.59	65.75	(8.84)	74.47	(0.12)	81.17	6.58	73.87	(0.72)
32	60.19	71.52	11.33	61.17	0.98	70.79	10.60	60.58	0.38
33	48.39	29.89	(18.50)	54.44	6.05	55.92	7.52	53.14	4.75
34	36.89	51.29	14.40	37.28	0.39	40.33	3.44	36.40	(0.49)
35	45.04	47.37	2.33	48.29	3.25	47.15	2.11	47.29	2.25
36	50.59	38.83	(11.76)	57.22	6.63	64.22	13.63	56.43	5.84
37	61.00	62.65	1.65	54.84	(6.17)	56.32	(4.69)	54.10	(6.90)
38	66.04	62.18	(3.86)	50.33	(15.71)	53.41	(12.63)	49.35	(16.69)
39	64.55	64.12	(0.43)	61.44	(3.11)	61.17	(3.38)	60.45	(4.10)
40	76.66	58.35	(18.31)	75.31	(1.35)	85.61	8.95	74.71	(1.95)

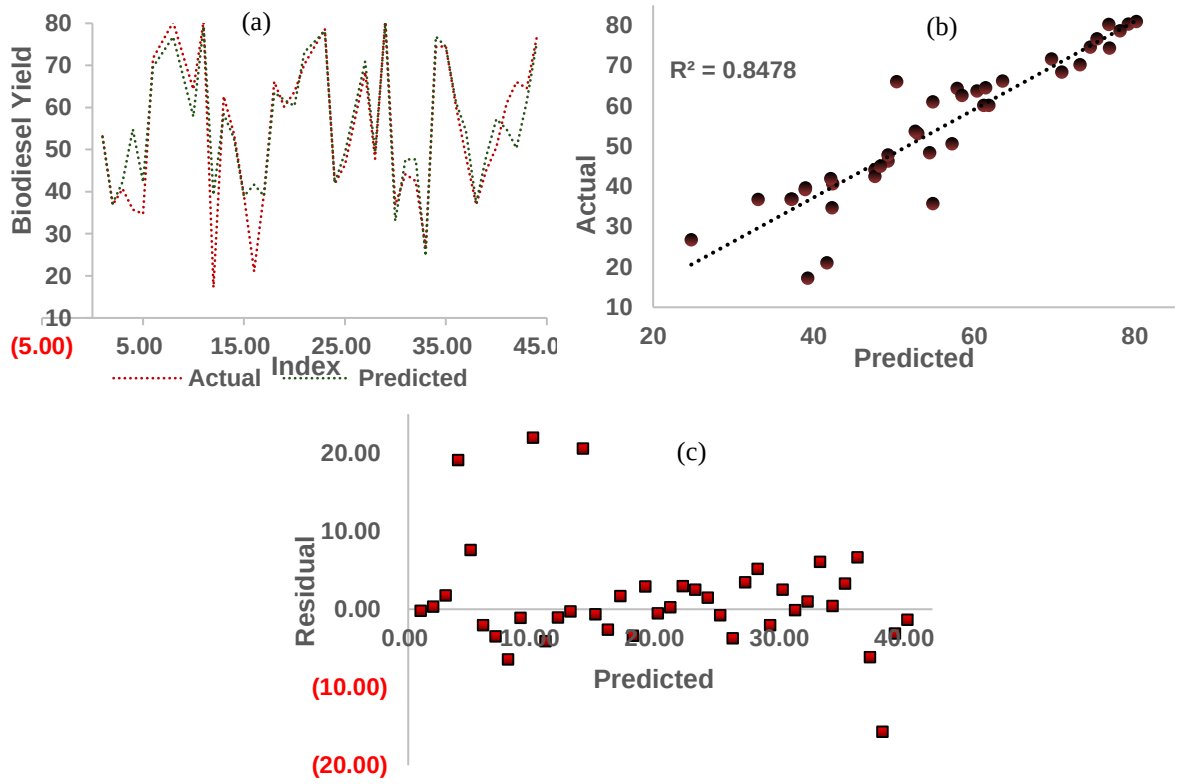

Figure 8: PSO model plots of biodiesel yield for (a) actual and predicted, (b) regression, and (c) residual errors

GA biodiesel model

The output of the RSM model was considered to evaluate the values of the fitness function for the GA routine available in the MATLAB Genetic Algorithm toolbox (Sivamani et al., 2018). This was carried out to obtain the optimum solution for the biodiesel yield as shown in Equation 9.

$$Y=53.545*A+1002*B-21.8349*C-170.996*D-41.7691*A*B-0.81158*A*C-4.36003*A*D-2.6875*B*C-30.9019*B*D+4.25822*C*D+4.26718*(A^2)-154.712*(B^2)+0.100338*(C^2)+8.0034*(D^2)+0.258824*A*B*C+0.278133*A*B*D+0.0479247*A*C*D+0.146772*B*C*D-0.531524*(A^2)*B-0.013234*(A^2)*C-0.010964*A^2*D^2+6.11122*B^2*A+0.00072717*C^2*A+0.0387787*D^2*A-0.78211*B^2*C+0.649904*B^2*D+0.0139687*B*C^2+0.560549*B*D^2-0.024915*C^2*D-0.075*C*D^2-0.0549138*A^3+13.2444*B^3+0.000567099*C^3-0.143144*D^3 \quad (9)$$

The numbers in this equation are the fitting parameters that go through the algorithm. The equation shows that the GA was successfully tested for the regression of the RSM at various MeOH: oil molar ratio, reaction time, reaction temperature, and catalyst quantity, to achieve the optimum biodiesel yield (Y). Also, the results of this search (GA) were compared with those of the RSM as shown in Table 10, to obtain the residual between the two data sets. The residual between the GA and RSM revealed a wide margin in some instances and a low margin in others. Figure 9a shows the plots of predicted and actual biodiesel yield when GA was deployed for the optimisation. Figure 9b shows the regression plot of the biodiesel yield with the GA method. The regression plot shows how dispersed the predicted data are from the actual, the R^2 value of this model is 0.8194, while the sum of residual error, MSE and RMSE are 5.48, 82.42 and 9.0621 respectively. Figure 9c shows the result of the residual error by comparing the residual and predicted data sets of biodiesel yield for the GA model. The figure showed large deviations to the positive compared to the negative and the maximum deviation to the positive and negative are 28 and -12, respectively.

FA biodiesel model

The simulation result of biodiesel yield using the FA model with the process conditions (Table 1) is given as an objective function in Equation 10. The numbers in this equation are the fitting parameters that went through the algorithm. Also, the results of this search (FA) were compared with those of the RSM as shown in Table 10, to obtain the residual between the two data sets. Figure 10a shows the model prediction compared with the actual biodiesel yield. The model was shown to perform creditably well as the match between the actual and predicted is approximately the same. Figure 10b shows the regression plot of the biodiesel yield when the FA method was deployed for the optimisation. The plot showed

the level of dispersion of actual data against the predicted data with an R^2 of 0.8478.

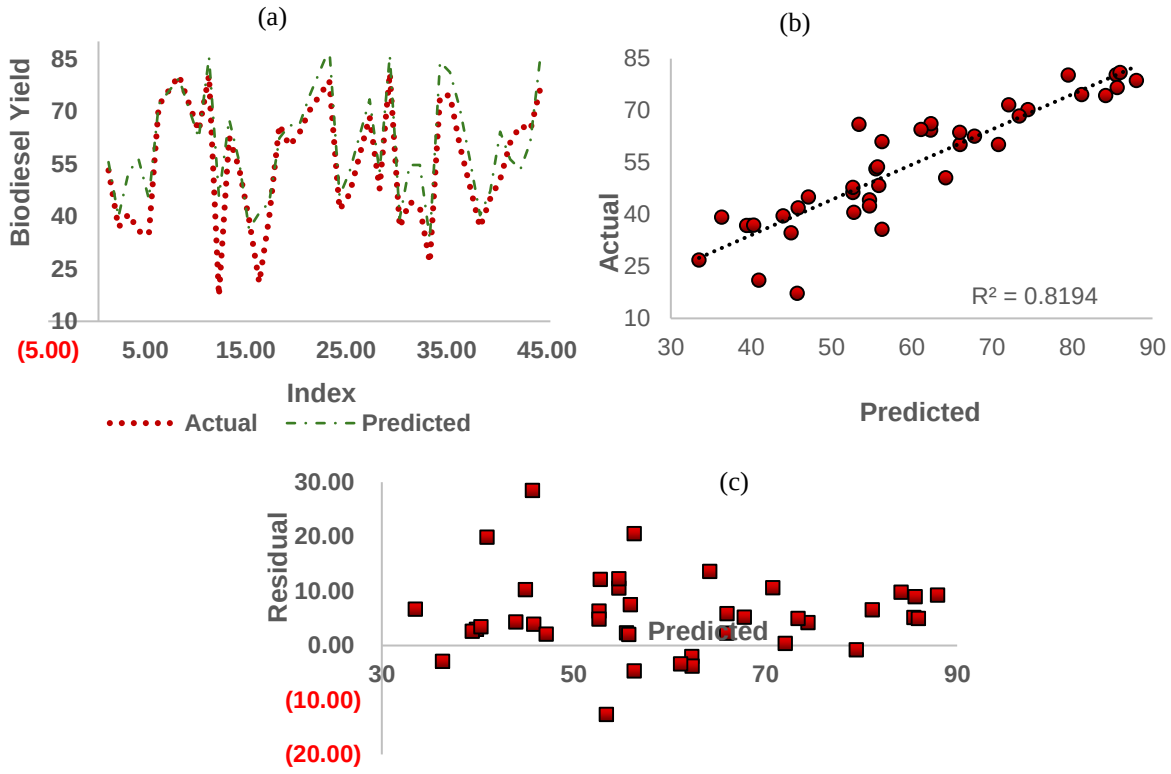

Figure 9: GA model plots of biodiesel yield for (a) actual and predicted, (b) regression, and (c) residual errors

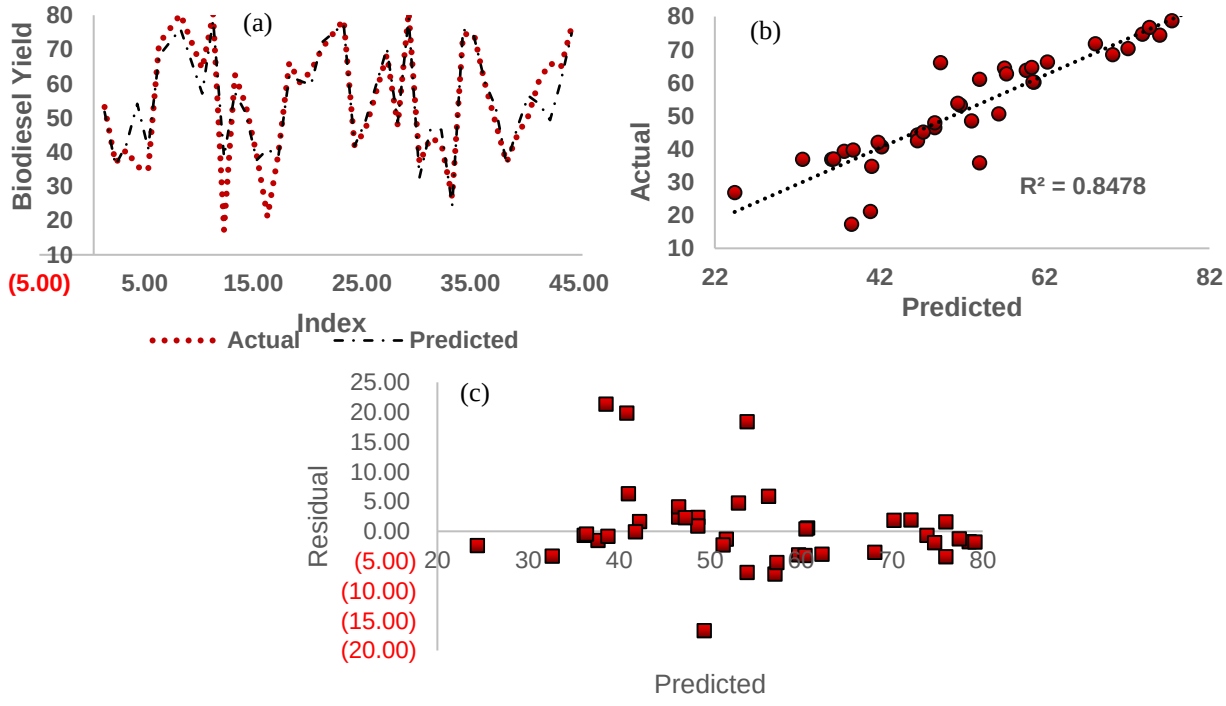

Figure 10: FA model plots of biodiesel yield for (a) actual and predicted, (b) regression, and (c) residual errors

$$Y=53.545*A+1000*B-21.8365*C-170.996*D-41.7691*A*B-0.811578*A*C-4.36003*A*D-2.68746*B*C-30.9019*B*D+4.25821*C*D+4.26718*A^2-154.712*B^2+0.100304*C^2+8.00336*D^2+0.258824*A*B*C+0.278133*A*B*D+0.0479247*A*C^2*D+0.146772*B*C*D-0.531524*A^2*B-0.013234*A^2*C-0.010964*A^2*D+6.11122*B^2*A+0.000727168*C^2*A+0.0387787*D^2*A-0.782108*B^2*C+0.6504*B^2*D+0.014*B*C^2+0.5606*B*D^2-0.024915*C^2*D-0.074711*C*D^2-0.0549138*A^3+13.1844*B^3+0.000567099*C^3-0.143144*D^3 \quad (10)$$

Figure 10c shows the residual error of the FA model by comparing the residual and predicted data sets of biodiesel yield. There are large deviations to the positive compared to the negative and the maximum deviation to the positive and negative are 25 and -15 respectively. Table 11a shows the maximum biodiesel yield solutions achieved before the 10th generation. As shown in the table, the yield follows a decreasing order of PSO, FA, ANN, and GA with conversion efficiencies of 95.28%, 95.27%, 95.20%, and 95.14% respectively. The metrics of the maximum generation cost function and average generation cost function show that the PSO and FA have approximately the same biodiesel yield efficiency and perform better than the GA. This could suggest that the PSO model performed slightly better than the remaining models in maximising the cost function. It could also be observed from the cost function comparison plot for the metaheuristic algorithms that the FA solutions of individuals' standard deviation in a generation converge to a singular solution quicker than PSO and GA. Due to this non-convergence of the model's performance using the cost function, it is necessary to consider the statistical analysis to determine the most efficient model. The models were further investigated for statistical consistency using R^2, MSE, RMSE, SRE, and AAD. The data obtained for each model for the statistical quantities are presented in Table 11b.

Table 11a: Performance metrics of the algorithms at 100th generation

	Models (%)			
Biodiesel yield metrics	**ANN**	**PSO**	**GA**	**FA**
Maximum generation cost function	95.20	95.28	95.14	95.27
Average cost function	94.26	94.25	94.95	94.27

Table 11b: Statistical measures for the models

Regression and error data for the biodiesel yield				
	ANN	**PSO**	**GA**	**FA**
R^2	0.8832	0.8478	0.8494	0.8478
MSE	105	46.553	42.105	48.758
RMSE	10.24695077	6.82297589	6.061180938	6.98269289
SRE	1.69	1.27	1.45	0.455
AAD	13.86	12.42	12.93	12.29

From the table (Table 11b), the R^2 for each of the models is >0.840 which indicates a good fit between the experimental and predicted data. The computed values of MSE, RMSE, SRE, and AAD are all low values which indicate a good fit and better performance of the models (Betiku et al., 2016). The PSO, GA, and FA showed lower values for MSE, RMSE, SRE, and AAD compared to those obtained from the ANN model as presented in the table. These findings suggest the superiority of the meta-heuristic algorithms over ANN in terms of predictability, reliability, high precision, and accuracy (Ighose et al., 2017; Ishola et al., 2019). The optimisation algorithm-derived models and machine learning model are optimised by maximising the biodiesel yield and minimising the operating conditions using grid search. The same set of low feature values was used for the grid search of the different models/mathematical expressions. The results of this study are presented in Table 12. The results of the multi-objective optimisation after learning the complex relationship between biodiesel and other inputs establish a better understanding of the process of converting WRF to biodiesel using an AKC-CEC catalyst to optimise the yield. The values in the table were validated by repeating the experimental procedure for the biodiesel production using the input parameters, in triplicates. This is necessary to enhance the reliability of the findings and to ensure alignment between predicted values and real-world outcomes. Thus, the biodiesel yields obtained under the optimal parameters and the percentage error between the actual and predicted biodiesel yield are also presented in Table 12. The results show that GA and FA consistently gave higher biodiesel yield compared to other models which is consistent with the performance in terms of the optimal input variables. This performance indicates that the GA and FA might be more robust at identifying optimal conditions for maximizing biodiesel production. However, when considering these results, it is crucial to weigh the computational complexity and resource requirements associated with each model. The practical considerations for the best of the model should also include cost, environmental impact, and scalability which should guide the selection of the optimal model for real-world applications. Overall, the GA and FA exhibit promising performance and highlight their optimisation capabilities in the implementation of optimal input variables for biodiesel production. The optimal input parameters within the given boundaries (Table 12), predicted and actual biodiesel yields as well as the percentage errors between the biodiesel yields, for each of the models are shown in Table 12.

Considering the optimal methanol: oil molar ratio shown in the table where the GA and FA proposed lower values compared to RSM, ANN, and PSO. This implies that the GA and FA are potentially more efficient in the utilization of methanol in the transesterification process compared to other models. Upon evaluation of the optimum reaction time for the input variable, both GA and FA proposed lower values, indicating faster processes compared to RSM, ANN, and PSO. Upon examination of the optimum reaction temperature for input variables, RSM provided a lower value compared to other models. While lower temperature may lead to reduced energy consumption which could also impact the reaction kinetics. Therefore, the choice of the optimal temperature

should consider the balance between energy efficiency and reaction rate. Also, upon evaluation of the optimum catalyst quantity for the input variable, both GA and FA models proposed higher values which shows these algorithms in effective and efficient mapping of the biodiesel yield to the features compared to other algorithms. This suggests that these algorithms prioritize higher catalyst amounts for achieving optimal biodiesel yields. The selection of the appropriate catalyst quantity should be evaluated in the context of cost, availability, and environmental considerations. In general, GA and FA showed better performance than other models with respect to input variables for biodiesel production. This observation suggests potential advantages of the GA and FA for industrial-scale biodiesel production, particularly, where a lower methanol: oil molar ratio and shorter reaction times could contribute to the increase in the efficiency and productivity of the process.

Table 12: Optimal parameters for the models

	Models				
Optimal Variables	**RSM**	**ANN**	**PSO**	**GA**	**FA**
Methanol: oil molar ratio (w/w)	12.07	13.00	11.67	10.33	10.33
Reaction time (h)	2.58	3.50	3.67	2.33	2.33
Reaction temperature (^oC)	89.60	96.50	94.21	95.00	95.00
Catalyst quantity (%, w/w)	5.06	4.00	4.00	6.44	6.44
Predicted response (Biodiesel yield (%))	82.75	89.98	77.99	99.00	99.00
Actual response (Biodiesel yield (%))	82.99	89.89	78.01	99.24	
Percentage error	0.29	0.10	0.03	0.23	

Table 13: Comparison analysis of relevant studies on biodiesel production maximisation

Feedstock	Optimisation methods	Alcohol: oil ratio	Catalyst type and loading	Temperature and reaction time	Yield (%)	References
Waste date seed oil	RSM	15:01	Magnetic solid acid, 1.5% (wt.)	55^{o}C, 47 min	91.4	Al-Mawali et al., (2021)
WCO	ML, T2FLS T1FLS ANFIS RMS	10:01	CaO derived from Ostrich eggshells, 1.5% (wt.)	65^{o}C, 90 min	96.7 96.8 96.4 97.5	Kumar et al., (2022)
WCO	DOE	12:01	CaO (eggshell), 2.5% (wt.)	60^{o}C, 2 h	94	(Erchamo et al., 2021)
Scenedesmus algal	DOE	11:01	CaO (waste), 1% (wt.)	60^{o}C, 3 h	92	Weldeslase et al., (2023)
WCO	RSM	14:01	Zn-CaO, 5% (wt.)	57.5^{o}C, 2 h	96.65	
WRF (With modified kaolinite clay with Cao from eggshells as the catalyst)	RSM ANN PSO GA FA	12.07:01 13.00:01 11.67:01 10.33:01 10.33:01	5.06% (wt) 4.00% (wt) 4.00% (wt) 4.00% (wt) 4.00% (wt)	90^{o}C, 2.58 h 97^{o}C, 3.5 h 94^{o}C, 3.67 h 95^{o}C, 2.33 h 95^{o}C, 2.33h	82.99 89.89 78.01 99.24 99.24	**This work**

Upon comparison of predicted biodiesel yield presented in Table 9, the data show a complete deviation of the RSM (82.75%) from the other models of ANN (89.98), PSO (77.99%), GA (99.00%), and FA (99.00%). However, there was a close match among the GA and FA models as they outperformed other models in this study. While the ANN

performed higher than the RSM, and the PSO was lower than the RSM, in terms of maximum biodiesel yield.

C. Fuel Properties of the Biodiesel

The FAME profile of the WRF biodiesel sample which includes retention time and peak area (%) is shown in Table 13b. The FAME present are cis-9-hexadecenoic acid, pentadecanoic acid, 9-octadecenoic acid, stearic acid, cis-13-eicosenoic acid, 22-tricosenoic acid, and erucic acid with percentage peak area of 0.76%, 6.41%, 71.32%, 4.60%, 0.09%, 12.32%, and 1.92%, respectively. These yielded a total percentage FAME composition of 97.42% which is above the 96.5% recommended by the ASTM (Ajala et al., 2019). The results also indicate that 9-octadecenoic acid (unsaturated fatty acid) has the highest FAME percentage composition of 71.32% in the WRF biodiesel. This further confirms the quality of the biodiesel produced as the presence of more unsaturated fatty acid yields a high oxidation and thermal stability (Ajala et al., 2020). The high unsaturated fatty acid also indicates a much slower deterioration rate and provides a long shelf-life of biodiesel. The high unsaturated fatty acid of the biodiesel is also responsible for the density, kinematic viscosity, and lower emission of HC, and CO samples also depend on the higher unsaturated chain (Ajala et al., 2019).

Table 13b: FAME profile of WRF biodiesel

Peak no	Retention time (min)	FAME profile	Molecular formula	Peak area (%)
1	14.078	cis-9-Hexadecenoic acid	$C_{16}H_{30}O_2$	0.76
2	14.284	Pentadecanoic acid	$C_{15}H_{30}O_2$	6.41
3	16.229	9-Octadecenoic acid	$C_{18}H_{34}O_2$	6.71
4	16.417	Stearic acid	$C_{19}H_{38}O_2$	4.60
5	18.481	cis-13-Eicosenoic acid	$C_{20}H_{38}O_2$	0.09
6	19.213	9-Octadecenoic acid	$C_{18}H_{34}O_2$	0.21
7	22.616	9-Octadecenoic acid	$C_{18}H_{34}O_2$	42.21
8	22.966	9-Octadecenoic acid	$C_{18}H_{34}O_2$	17.64
9	23.454	22-Tricosenoic acid	$C_{23}H_{44}O_2$	9.94
10	23.486	22-Tricosenoic acid	$C_{23}H_{44}O_2$	2.10
11	23.623	9-Octadecenoic acid	$C_{18}H_{34}O_2$	2.96
12	23.811	Erucic acid	$C_{22}H_{42}O_2$	1.92
13	23.911	9-Octadecenoic acid	$C_{18}H_{34}O_2$	0.86
14	23.961	22-Tricosenoic acid	$C_{23}H_{44}O_2$	0.28
15	24.174	9-Octadecenoic acid	$C_{18}H_{34}O_2$	0.73

IV. CONCLUSION

From the models investigated for the optimisation studies, GA, and FA excellently performed well, as the two models produced 99.00% (predicted) and 99.24% (actual) biodiesel yield. The optimal input variables that achieved this optimum yield are methanol: oil molar ratio of 10.33 w/w, reaction time of 2.33 h, reaction temperature of 95ºC, and catalyst quantity of 6.44% (w/w). This study confirms the validity of modern algorithms such as GA, and FA in exploring the best operating conditions to achieve optimum biodiesel yield. This optimisation approach served dual purposes: it modelled the system and found the optimal parameter set that satisfied the objective function. These purposes allow for a succinct performance comparison of the algorithms directly with RSM and ANN. Therefore, this approach addressed the potential limitations of ANN, particularly its tendency to overfit when trained on smaller datasets, which could lead to poor generalisation and suboptimal optimisation results as more data is introduced. Among the algorithms investigated GA and FA outperformed the PSO, and also outperformed the RSM and ANN. The GCMS analysis also confirmed that the synthesised biodiesel with 97.42% FAME composition.

AUTHOR CONTRIBUTIONS

E.O. Ajala: Conceptualisation, methodology, analysis, manuscript writing - original draft and revision. A.B. Ehinmowo: Methodology, analysis, manuscript writing - original draft. A.D. Oladipupo: Methodology, analysis, manuscript writing - original draft and revision. I.S. Opawoye: Methodology, manuscript writing - revision. A.M. Ndana: Analysis, manuscript writing - review and editing. D.A. Ariyoosu: Manuscript writing - revision.

REFERENCES

Ajala, E. O., Ajala, M. A., Afolabi, F. D., Ajala, J. O., Opawoye, S., & Ariyoosu, D. A. (2024). Waste-ram-fat as a Feedstock for Biodiesel Production using Heterogeneous Catalyst of Kaolinite-clay Impregnated Calcium-oxide from Chicken Eggshell. *Nigerian Journal of Technological Development*, *21*(4), 168–179.

Ajala, E. O., Ajala, M. A., Ayinla, I. K., Sonusi, A.

D., & Fanodun, S. E. (2020). Nano-synthesis of solid acid catalysts from waste-iron-filling for biodiesel production using high-free acid waste cooking oil. *Scientific Reports*, *10*(13256), 1–21.

Ajala, E. O., Ajala, M. A., Okedere, O. B., Aberuagba, F., & Awoyemi, V. (2019). Synthesis of solid catalyst from natural calcite for biodiesel production: Case study of palm kernel oil in an optimisation study using definitive screening design study of palm kernel oil in an optimisation study using definitive. *Biofuels*, *0*(0), 1–12.

Ajala, E. O., Ehinmowo, A. B., Ajala, M. A., Ohiro, O. A., Aderibigbe, F. A., & Ajao, A. O. (2022). Optimisation of CaO-Al_2O_3-SiO_2-$CaSO_4$-based catalysts performance for methanolysis of waste lard for biodiesel production using response surface methodology and meta-heuristic algorithms. *Fuel Processing Technology*, *226*(October 2021), 107066.

Albuquerque, M. C. G., Jiménez-Urbistondo, I., Santamaría-González, J., Mérida-Robles, J. M., Moreno-Tost, R., Rodríguez-Castellón, E., Jiménez-López, A., Azevedo, D. C. S., Cavalcante, C. L., & Maireles-Torres, P. (2008). CaO supported on mesoporous silicas as basic catalysts for transesterification reactions. *Applied Catalysis A: General*, *334*(1–2), 35–43.

Altherwi, A. (2020). Application of the firefly algorithm for optimal production and demand forecasting at a selected industrial plant. *Open Journal of Business and Management*, *8*, 2451–2459.

Antonio, D., Santisteban, O. A. N., Vasconcellos, A. De, Silva, A., Aranda, D. A. G., Vinicius, M., Jaeger, C., & Nery, J. G. (2018). Metallo-stannosilicate heterogeneous catalyst for biodiesel production using edible, non-edible and waste oils as feedstock. *Journal of Environmental Chemical Engineering*, *6*(July), 5488–5497.

Ardabili, S. F., Najafi, B., Alizamir, M., Mosavi, A., Shamshirband, S., & Rabczuk, T. (2018). Using SVM-RSM and ELM-RSM approaches for optimizing the production process of methyl and ethyl esters. *Energies*, *11*(11).

Banković-Ilić, I. B., Stojković, I. J., Stamenković, O. S., Veljkovic, V. B., & Hung, Y. T. (2014). Waste animal fats as feedstocks for biodiesel production. In *Civil and Environmental Engineering Faculty Publications* (Vol. 104, pp. 1–17).

Betiku, E., & Ajala, S. O. (2014). Modeling and optimization of Thevetia peruviana (yellow oleander) oil biodiesel synthesis via Musa paradisiacal (plantain) peels as heterogeneous base catalyst: A case of artificial neural network vs. response surface methodology. *Industrial Crops and Products*, *53*, 314–322.

Betiku, E., Odude, V. O., Ishola, N. B., Bamimore, A., Osunleke, A. S., & Okeleye, A. A. (2016). Predictive capability evaluation of RSM, ANFIS and ANN: A case of reduction of high free fatty acid of palm kernel oil via esterification process. *Energy Conversion and Management*, *124*, 219–230.

Betiku, E., & Taiwo, A. E. (2015). Modeling and optimization of bioethanol production from breadfruit starch hydrolyzate vis-a-vis response surface methodology and artificial neural network. *Renewable Energy*, *74*, 87–94.

Buchori, L., Anggoro, D. D., Tsaniya, F., Elyasa, M. B., & Noviariyono, E. (2019). The effect of catalyst loading on the biodiesel production from lard. *The 3rd International Conference of Chemical and Materials Engineering*, *1295*, 1–4.

Buchori, L., Widayat, W., Muraza, O., Amali, M. I., Maulida, R. W., & Prameswari, J. (2020). Effect of Temperature and Concentration of Zeolite Catalysts from Geothermal Solid Waste in Biodiesel. *Processes*, *8*(1629), 1–16.

Coello, C. A. C., Lamont, G. B., & Veldhuizen, D. A. Van. (2007). Evolutionary Algorithms for Solving Multi-Objective Problems. In D. E. Goldberg & J. R. Koza (Eds.), *Genetic and Evolution Computation* (2nd ed.). Springer.

Daniyan, I. A., Adeodu, A. O., Dada, O. M., & Adewumi, D. F. (2015). Effects of reaction time on biodiesel yield. *Journal of Bioprocessing and Chemical Engineering*, *3*(2), 6–8.

Dewangan, A., Mallick, A., Yadav, A. K., Ahmad, A., & Alqahtani, D. (2023). Combined effect of operating parameters and nanoparticles on the performance of a diesel engine: Response surface methodology- coupled genetic algorithm approach. *ACS Omega*, *8*, 24586–24600.

Dirik, M. (2023). Utilizing firefly algorithm-optimized ANFIS for estimating engine torque and emissions based on fuel use and speed. *Fuzzy Optimization and Modelling Journal*, *4*(2), 13–26.

Doroody, C., & Kiong, T. S. (2018). Performance comparison of FA, PSO and CS application in SINR optimisation for LCMV beamforming technique. *Wireless Personal Communications*, *103*(3), 2177–2195.

Erchamo, Y. S., Mamo, T. T., & Workneh, G. A. (2021). Improved biodiesel production from waste cooking oil with mixed methanol – ethanol using enhanced eggshell - derived CaO nano - catalyst. *Scientific Reports*, 1–12.

Fajuke, I. D., & Raji, A. K. (2022). Firefly algorithm-based optimization of the additional energy yield of bifacial PV modules. *Energies*, *15*(2651), 1–13.

Hajra, B., Sultana, N., Pathak, A. K., & Guria, C. (2015). Response surface method and genetic algorithm assisted optimal synthesis of biodiesel from high free fatty acid sal oil (Shorea robusta) using ion-exchange resin at high temperature. *Journal of Environmental Chemical Engineering*, *3*, 2378–2392.

Hasan, N., & Ratnam, M. V. (2022). Biodiesel production from waste animal fat by transesterification using H2SO4 and KOH catalysts: A study of physiochemical properties. *International Journal of Chemical Engineering*, 1–7.

Ighose, B. O., Adeleke, I. A., Damos, M., Adeola, H., Ernest, K., & Betiku, E. (2017). Optimization of biodiesel production from Thevetia peruviana seed oil by adaptive neuro-fuzzy inference system coupled with genetic algorithm and response surface methodology. *Energy Conversion and Management*, *132*, 231–240.

Ishola, N. B., Okeleye, A. A., Osunleke, A. S., &

Betiku, E. (2019). Process modeling and optimization of sorrel biodiesel synthesis using barium hydroxide as a base heterogeneous catalyst: Appraisal of response surface methodology, neural network and neuro-fuzzy system. *Neural Computing and Applications*, *7*, 4929–4943.

Kadi, M. A., Akkouche, N., Awad, S., Loubar, K., & Tazerout, M. (2019). Kinetic study of transesteri fi cation using particle swarm optimization method. *Heliyon*, *5*(July), 1–9.

Kolakoti, A., Jha, P., Mosa, P. R., & Mahapatro, M. (2020). Optimization and modelling of mahua oil biodiesel using RSM and genetic algorithm techniques. *Mathematical Models in Engineering*, *6*(2), 134–146.

Linganiso, E. C., Tlhaole, B., Magagula, L. P., Dziike, S., Linganiso, L. Z., Motaung, T. E., Moloto, N., & Tetana, Z. N. (2022). Biodiesel Production from Waste Oils : A South African Outlook. *Sustainability*, *14*(1983), 1–21.

Mandari, V., & Kumar, S. (2022). Biodiesel Production Using Homogeneous, Heterogeneous, and Enzyme Catalysts via Transesterification and Esterification Reactions: a Critical Review. *BioEnergy Research*, *15*, 935–961.

Mohamed, M. A., Diab, A. A. Z., & Rezk, H. (2018). Partial shading mitigation of PV systems via different meta-heuristic techniques. *Renewable Energy*, *130*(January), 1159–1175.

Moulita, R. N., Rusdianasari, & Kalsum, L. (2019). Converting waste cooking oil into biodiesel using microwaves and high voltage technology. *Journal of Physics: Conf. Series*, *1167*(012033), 1–10.

Nassef, A. M., Sayed, E. T., Rezk, H., Ali, M., Rodriguez, C., & Olabi, A. G. (2018). Fuzzy-modeling with particle swarm optimization for enhancing the production of biodiesel from Microalga. *Energy Sources, Part A: Recovery, Utilization, and Environmental Effects*, *00*(00), 1–10.

Ngige, G. A., Ovuoraye, P. E., Igwegbe, C. A., Fetahi, E., Okeke, J. A., Yakubu, A. D., & Onyechi, P. C. (2023). RSM optimization and yield prediction for biodiesel produced from alkali-catalytic transesterification of pawpaw seed extract: Thermodynamics, kinetics, and multiple linear regression analysis. *Digital Chemical Engineering*, *6*(November 2022).

Odetoye, T. E., Agu, J. O., & Ajala, E. O. (2021). Biodiesel production from poultry wastes: Waste chicken fat and eggshell. *Journal of Environmental Chemical Engineering*, *May*, 105654.

Rezk, H., Fathy, A., & Abdelaziz, A. Y. (2017). A comparison of different global MPPT techniques based on meta-heuristic algorithms for photovoltaic system subjected to partial shading conditions. *Renewable and Sustainable Energy Reviews*, *74*(August 2016), 377–386.

Sadeghiram, S. (2017). Bacterial foraging optimisation algorithm, particle swarm optimisation and genetic algorithm: A comparative study. *International Journal of Bio-Inspired Computation*, *10*(4), 275–282.

Sarantopoulos, I., Chatzisymeon, E., Foteinis, S., & Tsoutsos, T. (2014). Optimization of biodiesel production from waste lard by a two-step transesterification process under mild conditions. *Energy for Sustainable Development*, *23*(January 2018), 110–114.

Sivamani, S., Selvakumar, S., & Rajendran, K. (2018). Artificial neural network–genetic algorithm- based optimization of biodiesel production from Simarouba glauca. *Biofuels*, *7269*, 1–10.

Toldra-Reig, F., Mora, L., & Toldra, F. (2020). Applied sciences trends in biodiesel production from animal fat waste. *Applied Science*, *10*(3644), 1–17.

Tsai, J. T., Liu, T. K., & Chou, J. H. (2004). Hybrid Taguchi-genetic algorithm for global numerical optimization. *IEEE Transactions on Evolutionary Computation*, *8*(4), 365–377.

Watanabe, R. B., Ando Junior, O. H., Leandro, P. G. M., Salvadori, F., Beck, M. F., Pereira, K., Brandt, M. H. M., & de Oliveira, F. M. (2022). Implementation of the bio-inspired metaheuristic firefly algorithm (FA) applied to maximum power point tracking of photovoltaic systems. *Energies*, *15*(15), 1–15.

Yang, X.-S. (2011). Optimization Algorithms. In S. Koziel & X.-S. Yang (Eds.), *Computational Optimization, Methods and Algorithms* (pp. 13–31). Springer Berlin Heidelberg.

Yousef, B. A. A., Rezk, H., Abdelkareem, M. A., Olabi, A. G., & Nassef, A. M. (2020). Fuzzy modeling and particle swarm optimization for determining the optimal operating parameters to enhance the bio-methanol production from sugarcane bagasse. *Energy Research*, *April*, 4–6.